

Article

Polyester-Based Coatings with a Metal Organic Framework: An Experimental Study for Corrosion Protection

Nicoleta Plesu ^{1,*}, Lavinia Macarie ¹, Milica Tara-Lunga Mihali ¹, Bianca Maranescu ², Aurelia Visa ^{1,*} and Dorin Jurcau ³

¹ “Coriolan Dragulescu” Institute of Chemistry, 24 Mihai Viteazu Bv., 300223 Timisoara, Romania; lmacarie@acad-icht.tm.edu.ro (L.M.); tlmilica@acad-icht.tm.edu.ro (M.T.-L.M.)

² Faculty of Chemistry, Biology, Geography, West University of Timisoara, 16 Pestalozzi Street, 300115 Timisoara, Romania; bianca.maranescu@e-uvt.ro

³ Elkim Special SRL, 21Constantin cel Mare St., 300290 Timisoara, Romania; dj7office@gmail.com

* Correspondence: nplesu@acad-icht.tm.edu.ro (N.P.); avisa@acad-icht.tm.edu.ro (A.V.); Tel.: +40-256491818 (N.P. & A.V.)

Abstract: Polyester coatings containing metal-organic framework (MOF) corrosion inhibitors were studied for their ability to protect carbon steel. The polyester coating was synthesized in the laboratory using microwave (MW) radiation to polycondense soy fatty acids, phthalic anhydride, and pentaerythritol-type polyols. The incorporation of these inhibitors into the polyester coating altered the behavior of the carbon steel, resulting in enhanced corrosion protection compared with uncoated carbon steel and polyester alone. Polyester with a 49% oil content, prepared using fatty acids from soybeans, phthalic anhydride, and pentaerythritol synthesized under microwave irradiation, and with a content of 3 mM Mg(GLY), exhibited a notable enhancement in the anticorrosive properties of the alkyd coating. The inhibition mechanism of corrosion was investigated through electrochemical impedance spectroscopy analysis.

Keywords: polyester coating; corrosion; MOF; electrochemical impedance spectroscopy (EIS); paints



Citation: Plesu, N.; Macarie, L.; Tara-Lunga Mihali, M.; Maranescu, B.; Visa, A.; Jurcau, D. Polyester-Based Coatings with a Metal Organic Framework: An Experimental Study for Corrosion Protection. *J. Compos. Sci.* **2023**, *7*, 422. <https://doi.org/10.3390/jcs7100422>

Academic Editor: Francesco Tornabene

Received: 4 September 2023

Revised: 13 September 2023

Accepted: 7 October 2023

Published: 9 October 2023



Copyright: © 2023 by the authors. Licensee MDPI, Basel, Switzerland. This article is an open access article distributed under the terms and conditions of the Creative Commons Attribution (CC BY) license (<https://creativecommons.org/licenses/by/4.0/>).

1. Introduction

Among the methods used to protect metal surfaces against corrosion, the most commonly used involves polymeric compositions [1]. The typical polymeric compositions for anticorrosive protection of metal surfaces are made up of a system containing anticorrosive primer and enamel. Anticorrosive primers generally have a high volumetric pigment content (high VPC), which makes them porous and sensitive to moisture. That is why they must be protected from environmental factors by applying a layer of enamel. Anti-corrosion protection depends on not only the type of anti-corrosion pigments used, but also on the binders used and all the additives included in the composition of these products. In addition to anticorrosive pigments, there are various additives that are introduced into the film-forming compositions and which have an anticorrosive role (for example, different types of tannin, imidazoline derivatives, etc.). If the anticorrosive film-forming composition is a water base formulation, corrosion inhibitors must also be introduced. Otherwise, until the film deposited on the metal surface dries by evaporation of water, rust is produced. Such additives can be nitrates, borates, organic compounds with nitrogen, etc. The anticorrosive primer unusually contains anticorrosive pigments (zinc phosphate, ferrites, zinc powder, etc.). The most effective anticorrosive pigment in history was lead minium, which is now banned. These polymer films act as a barrier against aggressive agents. Metals are widely used in almost all industrial and agricultural fields, but because of exposure to the environment that can be more or less aggressive, over time they can undergo corrosion processes. As a result, the metal surface degrades, which affects the performance of the metal material and also their safety in use, to which are added substantial

financial losses. As a result, research is directed towards finding viable solutions to stop or limit corrosion processes. One of the most common and long-used methods to improve anti-corrosion protection is the formation of protective organic layers on the metal surface. As a disadvantage, the protection offered by organic layers is expensive, requiring constant replacement of the surfaces by painting; therefore, better alternatives are needed [1]. The type of organic compound used, the compactness and adhesion of the deposited layer dictate the quality of the protective layer and, as a result, its anti-corrosion protection [2–4]. Most organic coating systems include polymers (epoxies, acrylics, polyurethanes, etc.), and recently these have been modified to form a better protective barrier. The protective action of polymer films depends on the type of metal substrate, the method of treating the metal surface, the composition of the polymer films, the method of their deposition, the thickness of the deposited film and the degree of adhesion to the metal substrate. In recent years, the use of intelligent coatings capable of acting over time (self-healing and corrosion resistance) has been studied. Microcapsules using the double emulsion technique with similar action have been prepared [3,4]. The majority of intelligent coatings offer limited protection (the adherence of the newly formed film is crucial). The addition of active compounds (with anticorrosion action) to the coatings prevents the transfer of corrosive species to the metal substrate. Numerous inorganic or organic compounds (salts, acids, complexes, natural extracts, special polymers, etc.) or their combinations have been tested as corrosion inhibitors [5–11]. These only react intelligently to changes in pH and ionic strength and release active chemicals capable of protecting the metallic substrate against corrosion. By including lanthanide bis-phthalocyanine complexes, LnPc2 compounds, alkyd resin-based coatings anti-corrosion characteristics can be significantly increased [8]. The inhibition efficiency (IE) of alkyd limonite protection was ~98.4%, which reveals a promising action due to a synergism that increases the adhesive qualities, elongation character, and resistance to rapid deformation of the modified coatings [9]. This improvement in mechanical characteristics could be due to an increase in the surface interaction at the interface between the alkyd base matrix and the micro-sized limonite particles, which improves adhesion. For carbon steel pipelines, the recently created alkyd@LnPc2 nanocomposite coatings provide outstanding protection. To improve corrosion protection in aqueous polyacrylate coatings, ZnO and benzotriazole (BTA) were synthesized into microcapsules in a straightforward one-step process [12]. The ability of an NaNO₂ corrosion inhibitor containing microcapsules manufactured using the double emulsion process to prevent corrosion of metallic substrates has been investigated [13]. For example, NaNO₂ was chosen because of its superior performance in environments including concrete. Stable Fe₂O₃ and –FeOOH are facilitated by nitrite ions in the passive film, and the abietic acid shell deprotonates and becomes porous in alkaline solution, enabling the diffusion of the corrosion inhibitor [14]. The functionalized waterborne acrylic (WA) coatings prepared with CeO₂ nanoparticles or phosphate type compounds improved significantly the corrosion resistance of metallic substrates [15,16]. Conducting polymers (CPs) such polyaniline (PANI), poly-pyrrole (PPy), and polythiophene have recently been used as coating additives in coatings against corrosion. Epoxy microcapsules and PANI, nanofibers added to the coating create a self-healing epoxy/polyamide coating. Anti-corrosion performance was attributed predominantly to the controlled delivery of encapsulated epoxy healant and a dense network formation of PANI nanofibers in the matrix [17]. Modified ZnO nanoparticles and fluorinated ethylene propylene (FEP) were combined with an EP matrix to create a multifunctional super hydrophobic polymer capable of forming a coat with unique self-cleaning properties and a hydrophobic nature [18]. A super hydrophobic coating prepared through the incorporation of hydrophobic silica nanoparticles (SNs) into polymethyl methacrylate (PMMA), presents low corrosion current density (I_{corr}) (1.08 nA/cm²) compared with bare steel (29.7 μA/cm²), which is attributed mainly to the super hydrophobic nature of the surface [19]. Polyester-based coatings are affordable, have good chemical resistance, low physical absorption and good stability, and are used in preparing of coatings with anticorrosive action [20]. Graphene dispersed into a polyester resin provides a coating

with good barrier qualities [21,22]. The divalent magnesium ion (Mg^{2+}) presents a high charge to size ratio, resulting in a tendency towards bond polarization and covalent bond character, with a robust tendency to donor coordination [23]. As a result, the Mg^{2+} ions bind straightforwardly with oxygen from carboxylic or phosphonic ligands [24] and nitrogen based coligands [25].

As mentioned earlier, anticorrosive pigmented primers typically have a high pigment content, which can make them porous and susceptible to moisture. To protect them from environmental factors, it is necessary to apply a layer of enamel. In order to address the issues of low durability, adhesion, and protective capacity of alkyd pigmented coatings, we have found that the addition of an MOF as an additive can be beneficial. The ability of an MOF to gradually release the parent phosphonic acid over time leads to an improvement in the properties of the alkyd coatings.

In our previous research regarding the corrosive protection of phosphonic acids and metal phosphonates, we have observed their beneficial and retardant effects that are especially provided by an MOF. With the presence of nitrogen atoms and phosphate groups, it is expected that the presence of the small quantity of $Mg(GLY)(H_2O)_2$ in acidic and saline solution would have a positive effect on the passivation of iron and the compound would behave as a corrosion inhibitor. As a result, we added an MOF to some alkyd resins prepared by unconventional methods to obtain alkyds with anticorrosive properties [26,27]. In the present study, we prepared pigmented alkyd paints based on a medium oil polyester resin synthesized using a microwave synthesis reactor (MW), a technology we have developed in recent years. The paint contains the same content of pigment (in our case TiO_2) and a variable content of metal phosphonate $Mg(GLY)(H_2O)_2$ —manganese phosphonate metal organic framework (MOF). These allow the formation of films by oxidative cross-linking. Their anticorrosive performance in a saline environment was investigated for carbon steel by potentiodynamic techniques and impedance spectroscopy. In accordance with the known information on MOFs and because of the properties that result from the structures of these compounds, we investigate whether adding an MOF to an alkyd paint will have an inhibitory effect on corrosion.

2. Materials and Methods

2.1. Materials

All chemicals were obtained from commercial sources and used without further purification. The two major ingredients were a polyhydric alcohol (or polyol) and a polybasic carboxylic acid given the term “alkyd”. The notation and some characteristics of the prepared Alkyd with MOF additive are presented in Table 1. The overall structure of $Mg(GLY)$ can be envisioned as a 2D layered motif. Each individual layer is formed by $Mg-O$ (phosphonate) bonds, forming 16-membered rings. The coordination geometry of the Mg center is a distorted octahedral surrounded by six Mg-O bonds, four from phosphoric acid and two from water molecules [26,27].

Table 1. The characteristics of the tested coating.

No.	Sample	Pigment Content VPC %	MOF, mM	MOF Structure Mg(GLY)	Thickness, μm
1	Fe	25.76 ± 0.15	-		103 ± 7
2	Alkyd	25.76 ± 0.09	-		101 ± 3
3	Alkyd1	25.76 ± 1.30	1		101 ± 2
4	Alkyd2	25.76 ± 0.98	2		105 ± 6
5	Alkyd3	25.76 ± 1.41	3		104 ± 2
6	Alkyd4	25.76 ± 0.64	4		101 ± 4

2.2. Synthesis of MOF Additive-Mg(GLY)

All reagents were provided by Sigma-Aldrich and were used without further purification, except the bi-distilled water. The $Mg(GLY)$ was synthesized in our laboratory,

according to the literature and our previous work [26,27] starting from $\text{MgSO}_4 \cdot 7\text{H}_2\text{O}$ and *N,N*-bis (phosphonomethyl)glycine acid using hydrothermal conditions at 80 °C. The structure of Mg(GLY) is presented in Table 1.

2.3. Preparation of Paint

The paint was obtained by dispersing a pigment (TiO_2) into polyester resin dissolved in an aliphatic hydrocarbon solvent. The volumetric pigment concentration (VPC) chosen was low (~25.76%). The dispersion was carried out on a KADY® LT2000 (UK) type dispersion mill to obtain homogeneous dispersion of the pigment. The MOF was added to this composition in different concentrations and its performance as a corrosion inhibitor was tested. The amount of added MOF varied from 1, 2, 3 to 4 mM/100 g resin, and the given quantity was dispersed well in the pigmented polyester resin by ultrasound (Ultrasonic processing was performed at 36.24 kHz) [1b]. The paint forms the film by evaporating the solvent and then by oxidative cross-linking, with the help of a siccative mixture (0.05–0.8%) used in the final formulation. The main characteristics of the alkyd-type coating are presented in Table 2.

Table 2. Characteristics of synthesized liquid polyester resin and prepared alkyd-type coating.

Nr. Crt.	Technical Specifications	Determined Value	Method
Liquid polyester resin			
1	Appearance	Homogeneous viscous fluid	visual
2	Content in non-volatile substances, 2 h, 120 °C	65.4 ± 2	SR EN ISO3251:03
3	Flow time, DIN cup 4 mm, 20 °C, sec	85	DIN method 53211
4	Density, 20 °C, gr/cc	1.21	SR EN ISO2811-1:02
Alkyd-type coating			
1	Appearance	homogeneous film	visual
2	Type of drying at 20 °C, 1 h	A	
3	Type of drying at 20 °C, 2 h	A	STAS 2875-75
4	Type of drying at 20 °C, 24 h	D	
5	Erichsen Elasticity, mm,	7.5	ISO 1520:2006
6	Adhesion, 2 mm grid, adhesion value	2	SR EN ISO2409:2013
7	Flexibility, mm	3	SR EN ISO1519:2011
8	Dry film thickness, μm	45	ISO 2808:2020
9	Resistance to direct-impact, 0.5 kg, cm	30	SR EN ISO6272-1:2012
10	Hardness Persoz, sec	158	SR EN ISO1522:2007
11	Degree of gloss angle of 60°, %	91	ISO 2813:2014
12	Resistance to mineral oil, 2 h	Very good	SR EN ISO2812-2:2007
13	Resistance to water, 2 h	Very good	SR EN ISO2812-2:2007

2.4. Sample Preparation and Coatings Characterization

The carbon steel substrate was previously degreased with alcohol, sanded, rinsed with water and acetone, and finally dried in air before the experiments. The chemical composition of the substrate carbon steel used was C: 0.20%, Mn: 0.45%, P: 0.04%, S: 0.05%, with the balance being Fe. The steel was purchased from EPI Sistem (Brasov, Romania). The coatings were painted by the roll-coating method at ambient temperature (method GB/T1727.92). The samples were cured at room temperature (rt) for 24 h before measurement. The notations and characteristics of the tested coating are presented in Table 1. The alkyd-type coatings deposited on the surface of the electrodes had a thickness of $\sim 100 \pm 10 \mu\text{m}$. Corrosion measurements were performed on carbon steel specimens coated with alkyd resin containing different contents of MOF. Corrosion monitoring was carried out in immersion tests in 3.5 wt. % NaCl solution in open air, at room temperature. The experiments were performed in triplicate, the minimum number required to obtain a standard deviation. The coatings obtained were continuous, adherent to the metal surface and did not show cracks. The 400 mL corrosion (Autolab, Methrom) cell was used to

measure the corrosion properties of the coated circular samples. The exposed surface area of the working electrode (coated samples) was 0.785 cm^2 . The holder is made of Delrin with a Viton seal. Two inox bars were used as contra electrodes (CE). The reference electrode (RE) was Ag/AgCl (3 M KCl).

2.4.1. Open Circuit Potential (OCP)

Open Circuit Potential (OCP), also known as zero-current potential, corrosion potential, equilibrium potential, or rest potential, is a passive technique frequently used to determine a system's resting potential. The samples were kept under open circuit potential conditions for 1 h, to stabilize the electrode potential in saline 3.5% NaCl. The tests were carried out in triplicate.

2.4.2. Electrochemical Impedance Spectroscopy (EIS) Measurements

Experiments with EIS were also employed to investigate the corrosion process. EIS was conducted using the FRA2 impedance module and an Autolab 302N potentiostat/galvanostat. The tested frequency range was between 0.01 Hz and 100 kHz, and the sinusoidal potential amplitude was 10 mV. All the measurements were performed at room temperature in a typical one-compartment, three-electrode cell with two inox counter electrodes and an Ag/AgCl (3 M KCl) reference electrode. The working electrode's exposed surface area during the electrochemical studies was 1 cm^2 . At open circuit potentials, electrochemical impedance spectra were recorded, with 3.5% NaCl serving as the supporting electrolyte. ZView-Scribner Associated Inc. software (non-linear least squares approach) was used to fit the experimental data to a suitable electrical equivalent circuit (EEC). The tests were carried out in triplicate.

The water uptake tests were performed in triplicate based on the EIS data, and the error bars represent the standard deviation. For water absorption (W), the EIS spectra were recorded after one h and 120 h.

2.4.3. Optical Microscopy

Optical Microscope Zeiss Stemi 508 was used to exam the surface morphologies of the coated samples *ex situ*, before and after the corrosion investigations.

3. Results

The reaction between polyols and organic acids for polyester synthesis has practical applications, particularly in the production of polyesters and polymer plasticizers. This reaction typically occurs at high temperatures, resulting in significant energy consumption. Therefore, any new technology that can reduce energy consumption is beneficial for the industry. Polyesterification is an equilibrium reaction and is influenced by various factors, including the concentration of raw materials, the type and concentration of catalyst, the polarity of the reaction medium, the mode and intensity of agitation to ensure optimal reactant contact, the working temperature, and the chosen technological system. Economically viable production of esters and polyesters requires carboxylic acid-alcohol reactions in the molten state, at high temperatures, without the presence of strong acids that can induce secondary reactions and without the use of solvents. Esterification of acids with alcohols is a reversible reaction with a well-established mechanism [28,29].

The reaction times reported in the literature for polyesterifications vary significantly. Generally, uncatalyzed syntheses occur within 15–25 h, while catalyzed syntheses occur within 5–10 h. The duration of the reaction depends on factors such as the nature of the reactants, their proportions, the presence of a catalyst, stirring, the thermal conditions, and pressure. Prolonging the reaction time at a specific temperature may negatively affect the molecular weight as it can lead to secondary reactions that reduce the weight. In industrial syntheses, it is often preferred to extend the reaction time rather than using a catalyst that could compromise the quality of the polyester [30–33]. Based on experimental data, it has been found that the reverse reactions in the esterification process can be ignored at

temperatures below 180 °C and/or conversions lower than 95%. However, if a commercial process requires very high conversions, the reverse reactions cannot be neglected. The thermodynamically controlled phase, which is usually the longest part of an industrial polyesterification process, can be significantly shortened by applying a vacuum to accelerate water removal. For instance, a conversion of 99%, with an acid value of 5 mg KOH/g, can be achieved by reacting 5.97 mol of adipic acid with 6.52 mol of 1,3-butane diol in the presence of 0.2% dibutyltin oxide at 215 °C in 14.8 h. This time includes 2 h for heating to 215 °C, 1.9 h for kinetically controlled esterification at 94.5% conversion (acidity index 25 mg KOH/g), and 10.9 h for the thermodynamically controlled process at 99% conversion (acidity index 5 mg KOH/g). By conducting the latter part under a vacuum of only 60 Torr, the reaction can be completed in just 2.3 h, resulting in a total reaction time of 6.2 h. This is less than half the time required at normal pressure. Applying a vacuum at the beginning of the reaction does not provide any benefits, as it does not increase the rate of the kinetically controlled process. Moreover, it is challenging to maintain the vacuum as most of the initially generated water is distilled [31]. Considering all these aspects, the polyester was synthesized under microwave irradiation using soybean fatty acids, phthalic anhydride, and pentaerythritol (Oil length: 49%, Phthalic anhydride: 34.5%). Figure 1 illustrates the temperature time profile and evolution of the acidity index during MW-assisted polycondensation.

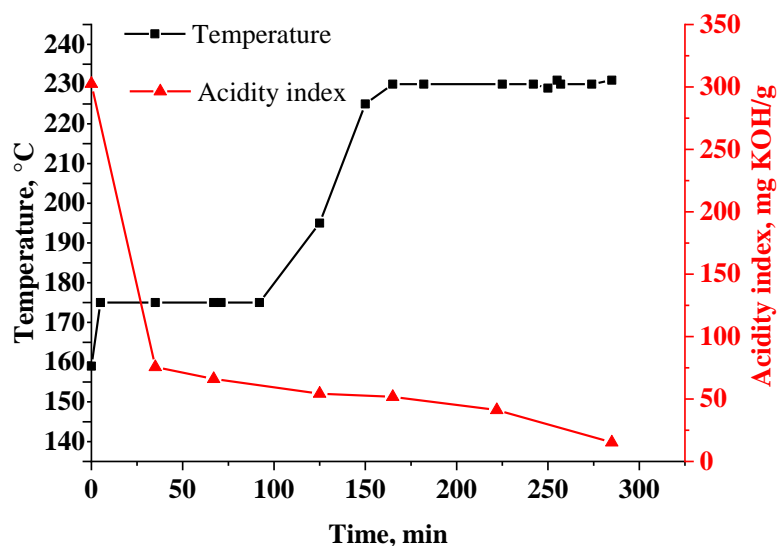


Figure 1. Temperature time profile and evolution of acidity index during MW-assisted polycondensation.

Alkyd resins with a medium oil content typically require an oil concentration range of 40% to 55%, which is also the case for our study. These resins dry quickly and exhibit a high level of gloss. They can be dissolved by aliphatic solvents such as white spirit, as well as stronger solvents like xylene or toluene. Based on experimental data, the conversion calculated using the acidity index was determined to be 93.89%. The resulting polyester resin is a homogeneous viscous liquid with a non-volatile substance content, Gardner color of 5, acidity index of 6.8 mg KOH/g, and a refractive index of 1.5040.

Polyester resin (alkyd) samples were prepared and characterized at SC ELKIM SPECIAL SRL, Timisoara. The resin was based on soy fatty acids, phthalic anhydride and polyols of the pentaerythritol type (Oil length: 49%. phthalic anhydride: 34.5%) in a MW reactor (MW-2000, 0~1800 W, 2450 + 50 MHz, with mechanical stirrer). The characteristics of the polyester resin are reported in Table 2.

Table 2 presents additional characteristics of the synthesized polyester resin (liquid polyester resin). Microwave-assisted transformations often involve rapid heating, which can lead to modified distributions of reaction products compared with conventional heating methods, such as reflux with classical oil bath heating. This is due to the complex temperature-dependent kinetics profiles that control the reaction product distribution.

Microwave-assisted chemical reactions at optimized temperatures have been shown to result in fewer secondary products compared with conventional heating conditions. In our case, the determined molecular weight averages were $2096 \text{ g}\cdot\text{mol}^{-1}$ for weight-average molar mass (Mw), $3986 \text{ g}\cdot\text{mol}^{-1}$ for number-average molar mass (Mn), and a polydispersity index (PID) of 1.91. The relatively narrow molecular weight distribution of the alkyd resin obtained under MW irradiation suggests that MW-assisted synthesis in this case reduces the formation of side reactions. All the characteristics determined for the alkyd-type coatings, as presented in Table 2, indicate that this alkyd resin is suitable for use as a coating. The addition of MOFs to paint formulations is expected to enhance the anticorrosive properties of the coatings. The open circuit potential was measured over a period of 1 h to determine the stable steady-state potential (Figure 2).

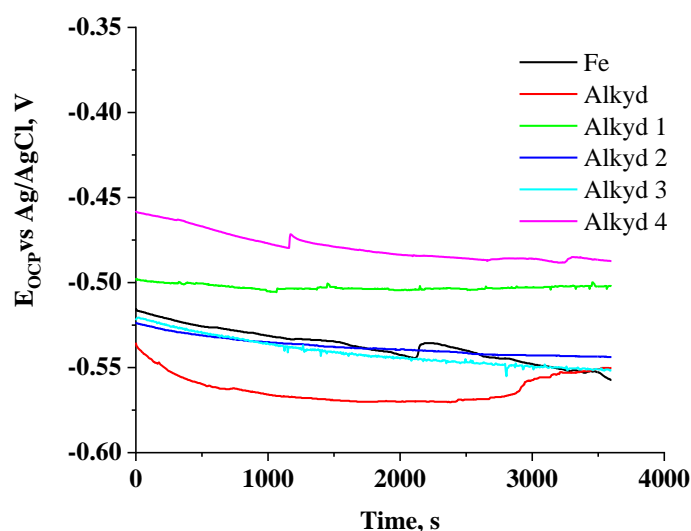


Figure 2. Variation in OCP potential with immersion time for carbon steel without alkyd coating (Fe), with alkyd coating and with alkyd coating and various Mg(GLY) contents (Alkyd 1, Alkyd 2, Alkyd 3 and Alkyd 4) immersed in 3.5% NaCl solution.

The OCP values for carbon steel decrease after 3600 s immersion in chlorine in saline solution; hence, the breakdown of the passive oxide layer generated at the sample surface (electrodes) takes place. The OCP values initially decrease within the first 500 s due to the attack of aggressive chloride ions, which can penetrate the metallic surface through existing pores in the coating (Figure 1). After this first period, a partial protection of the surface takes place due to the blocking of the existing pores and cracks by corrosion products, leading to potential stabilization. The MOF allowed small drops in OCP potential, and a constant value was more quickly reached, which gives qualitative information about their beneficial action as an anticorrosive additive. The shorter time required for OCP stabilization on carbon steel coated with alkyd with Mg(GLY), compared with when it is absent, suggests the formation of an enhanced protective layer on the metal surface. Monitoring the open circuit potential (OCP) over time provides information about the stability of the coating in the corrosive solution. These results indicate that MOFs (metal-organic frameworks) bring improvements in the corrosion protection of iron in saline media. Considering the nature of MOFs, they have the ability to eliminate free phosphonic acid through hydrolysis, providing corrosion protection by binding acid groups to the iron surface and trapping cations from the solution [27]. Comparing our results with the protective properties of paint systems, studies in the literature have shown a lower corrosion rate for alkyd paint compared with coatings based on butyl acrylate methyl methacrylate copolymers [2] or polyester graphene coatings [21]. Additionally, the use of MOFs as corrosion inhibitors demonstrates higher inhibition efficiency than titanium phosphates $\text{Li}_{0.5}\text{M}_{0.25}\text{Ti}_2(\text{PO}_4)_3$ (where M = Mn, Co, and Ni) added in alkyd resin films applied to a carbon steel substrate in a 3.5% sodium chloride solution [11]. MOFs provide comparable inhibition efficiency to

coatings with lanthanide bis-phthalocyanine complexes [8]. Electrochemical impedance spectroscopy (EIS) is a non-destructive testing method that provides valuable quantitative and qualitative corrosion data. In order to compare the corrosion behavior of the coatings, EIS experiments were conducted and the obtained data were analyzed using equivalent circuit models (Figure 3c). The Nyquist plots (Figure 3a) provide information about the electron transfer process. A larger radius of the semi-circular arc indicates higher resistance and more difficult electron transfer. Comparing the coated samples with the uncoated carbon steel, the diameters of the arcs for the coated samples are larger, indicating higher corrosion resistance. The order of decreasing corrosion resistance is as follows: Alkyd 3 > Alkyd 4 > Alkyd 2 > Alkyd 1 > Alkyd > Fe. The Bode plots presented in Figure 3b illustrate the impedance vs. frequency, and phase degree vs. frequency. The module of impedance ($|Z|$) also gives information about the corrosion process. A less protective coating presents a low $|Z|$ value, which means low resistance of the coating and high capacitance. The depressed capacitive loop observed in the Nyquist plots is due to surface roughness. The variation in the impedance values in the Bode modulus plots is consistent with that of the semicircle diameter in the Nyquist plots.

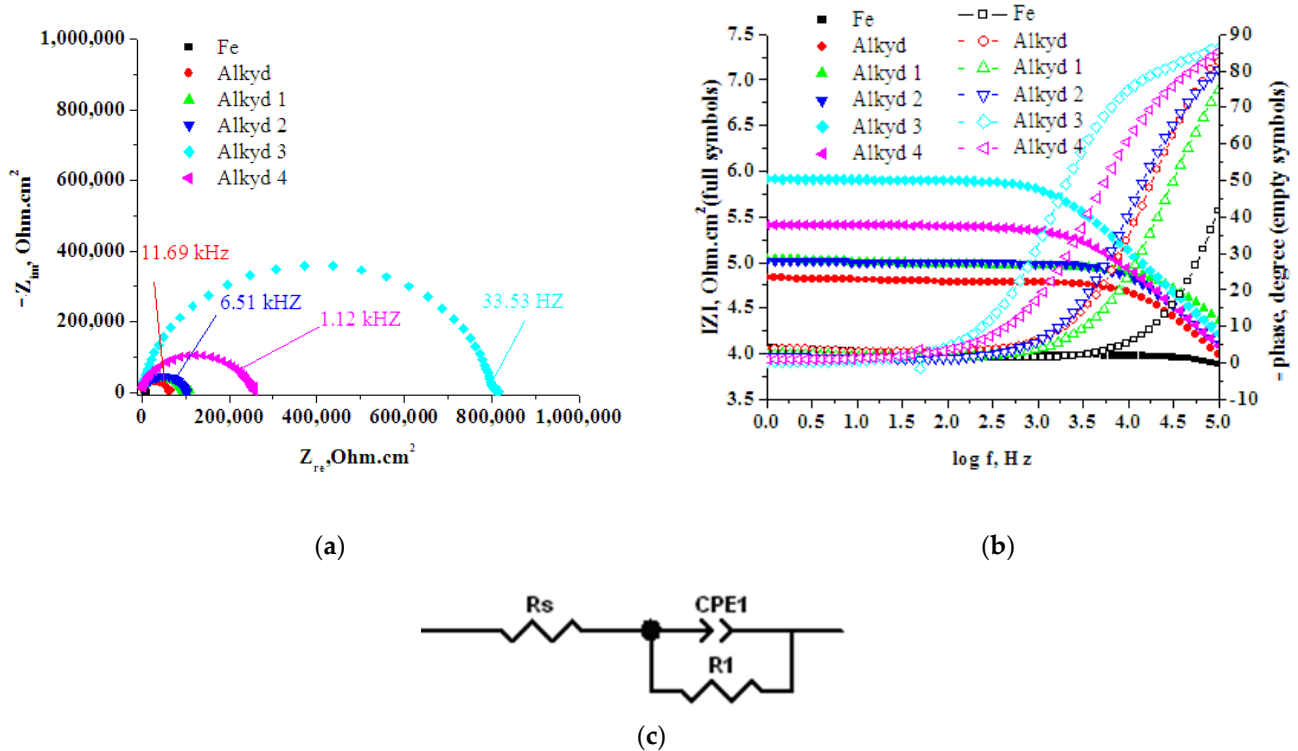


Figure 3. (a) Complex plane Nyquist plots; (b) Bode plots for uncoated and coated carbon steel immersed for 1 h in 3.5% NaCl solutions; and (c) equivalent circuit model (EEC).

In the Nyquist diagrams, an increase in the size and different levels of the diameter of the capacitive loop were observed, depending on the type of alkyd coating and the content of alkyd with MOFs. This indicates a reduction in the corrosion. The resistance of the coating, estimated from the impedance module ($|Z|$) at lower frequencies, also indicates a decrease in corrosion resistance. The $|Z|$ values of alkyd and alkyd with MOF content are higher than that of bare steel, suggesting that the presence of an MOF in the alkyd coating hinders the transport of electrolyte through the micropores of the coating to the metal surface. In the high-frequency region (between 1 kHz and 100 kHz), the incomplete capacitive semi-circle in the Nyquist plots arises from the non-uniform distribution of current on the electrode surface. The Bode magnitude plot displays a linear slope close to 1, and the phase angles reach their maximum values, indicating a capacitive behavior. In the intermediate frequency range (10^{-1} kHz) and at low frequencies (0.1^{-10} Hz), the

$\log |Z|$ values are in the range of 4.8 to 6 $\Omega \cdot \text{cm}^2$, and the $|Z|$ vs. frequency remains constant. For Alkyd 3 and Alkyd 4, the $\log |Z|$ values at a fixed frequency of 0.1 Hz, which usually corresponds to the polarization resistance of the alloys, lie between approximately 5.5 and 6 $\Omega \cdot \text{cm}^2$. At the same frequency, the $\log |Z|$ values of Alkyd and Alkyd 1 are about 4.8 to 5 $\Omega \cdot \text{cm}^2$, indicating that the corrosion resistance of Alkyd and Alkyd 1 is lower than that of Alkyd 3. Alkyd 3 exhibits, over a broad frequency range, capacitive behavior with phase angles close to -90° and high $|Z|$ values in the low-frequency region. The Nyquist plots in Figure 3a display different capacitive semiarcs, with the alkyd and Alkyd 1 and 2 coatings exhibiting capacitive semiarcs with much smaller diameters compared with Alkyd 3. It is also evident that the diameters of the capacitive semiarcs of the alkyd coatings depend on the MOF content. The MOFs used in this study offer various π -system topologies and functional groups, and these compounds have previously been investigated for their anticorrosive properties. The quality of the deposited layer on the metal surface depends on the concentration of MOF added to the alkyd resins. The magnitude $|Z|$ of the Alkyd 3-coated carbon steel is approximately 50% greater than that of the uncoated metallic substrate. The EIS data were fitted to an electrical equivalent circuit (EEC), as shown in Figure 3c, which includes one-time constants for the uncoated and coated carbon steel samples after 1 h of immersion. The electrical circuits consist of the solution resistance (R_s), the charge transfer resistance across the metal surface (R_1), and the double-layer capacitance between the metal surface and solution interface (C). Due to non-ideal behavior resulting from surface porosity and pore distribution, a constant phase element (CPE1) was used to replace the pure double-layer capacitor [33–36]. The electrical elements of the circuits closely fit the EIS data with the proposed model with the uncertain parameters R_s , R_1 , and CPE1-T. EEC was also used to model the corrosion process of Mg(GLY) in saline media [27]. The chi-square (χ^2) values were calculated to determine the quality of the equivalent circuit fitting. A value of $\chi^2 < 10^{-3}$ was obtained for all data, indicating a good agreement with the experimental data (Table 3). For all samples of alkyd with Mg(GLY) content, the R_1 values tended to increase with the Mg(GLY) concentration, surpassing those of alkyd alone, indicating the formation of a higher quality coating on the iron surface. This increase in corrosion resistance can be attributed to two factors. The first is the ability of Mg(GLY) and GLY to complex with Fe^{2+} cations generated from the attack of aggressive species in the corrosive environment through their carboxylic and phosphonic acid groups, respectively. This complexation helps to seal the pores in the coating. Secondly, the phosphonic groups can bind to the metal surface in a mono, bi, or tridentate manner, enhancing the adhesion of the deposited polyester layer. Among the samples, Alkyd 3 exhibited the highest R_1 value, indicating the formation of a more effective and compact coating on the iron surface. At Mg(GLY) concentrations of 1 mM and 2 mM in Alkyd, the R_1 values were higher than alkyd alone but lower than Alkyd 3. This suggests the release of free phosphonic acid, but in quantities insufficient to form a strong and dense protective coating on the iron surface. Additionally, the lower R_1 values obtained for Alkyd 4 indicate that at higher concentrations, the quality of the coating is compromised, resulting in a more porous coating, as supported by the optical image of the coating surface.

Table 3. Electrochemical parameters for carbon steel, after 60 min immersion in 3.5% NaCl solutions without and with alkyd coating.

Sample		EIS			
SD *	χ^2	$R_1, \Omega \cdot \text{cm}^2$	CPE1-T, $\text{F}/\text{cm}^2/\text{s}\varphi^{-1}$	CPE1-P, φ	IE, %
Fe	0.0041	$1.01 \times 10^4 \pm 0.91 \times 10^2$	$7.19 \times 10^{-6} \pm 0.656 \times 10^{-9}$	0.37 ± 0.03	-
Alkyd	0.007	$1.02 \times 10^5 \pm 1.03 \times 10^1$	$4.47 \times 10^{-10} \pm 5.14 \times 10^{-13}$	0.87 ± 0.04	90.06 ± 0.12
Alkyd1	0.0024	$2.49 \times 10^5 \pm 3.42 \times 10^1$	$2.22 \times 10^{-10} \pm 9.20 \times 10^{-12}$	0.9 ± 0.03	95.94 ± 0.34
Alkyd2	0.0014	$3.12 \times 10^5 \pm 0.91 \times 10^2$	$2.46 \times 10^{-10} \pm 0.78 \times 10^{-13}$	0.89 ± 0.01	96.76 ± 0.72
Alkyd3	0.0003	$3.51 \times 10^5 \pm 4.16 \times 10^2$	$2.55 \times 10^{-9} \pm 3.96 \times 10^{-14}$	0.91 ± 0.01	97.12 ± 0.91
Alkyd4	0.0057	$1.59 \times 10^5 \pm 9.03 \times 10^3$	$3.17 \times 10^{-10} \pm 0.526 \times 10^{-11}$	0.52 ± 0.03	93.64 ± 0.54

* SD standard deviation.

The lowest CPE1-T value was obtained for the Alkyd 3 sample, which indicates the formation of a thicker and more compact protective coating on the metallic surface. The increase in CPE1-T values observed for all the alkyd samples can be attributed to an increase in the dielectric constant and/or a decrease in the thickness of the electrical double layer. This further supports the idea that the presence of a minimum amount of free phosphonic acid, generated by acid hydrolysis, is necessary for the formation of a compact and protective coating on the metal surface. The deviation from ideal capacitive behavior depends strongly on the state of the surface and is expressed by the CPE1-P exponents. The values are in the range 0.52–0.98 (Table 3). A lower value indicates an increased effect due to surface disorder, adsorption, roughness, pore size and distribution. The obtained values are in accordance with the calculated roughness for coatings based on the surface images recorded with the optical microscope. The corrosion efficiency IE determined from the EIS data (Equation (1)) reveals an Mg(GLY) additive action as good as that observed for alkyd-based protective paints for steel petroleum structures incorporating natural limonite pigment [7] and one better than that obtained for alkyd resin coatings containing titanium phosphates or alkyd@lanthanidebis-phthalocyanine nanocomposite coatings [8,11] (Table 4).

$$IE = \frac{(R_{1i} - R_1)}{R_1} \times 100 \tag{1}$$

where R_{1i} and R_1 represent the polarization resistance for coated and uncoated iron surfaces, respectively.

Table 4. Alkyd coatings in the literature.

Coating	Substrate	IE %	Ref
1 Alkyd-based protective paints for steel petroleum structures incorporating natural limonite pigment	Steel in 5% NaCl	98.4	[7]
2 alkyd@lanthanidebis-phthalocyanine nanocomposite coatings alkyd@HoPc2	carbon steel pipelines in 0.5 HCl	87.4	[8]
3 Alkyd with 20% [poly(aniline-co-o-toluidine) Fe ₃ O ₄] MNPs	carbon steel (C101) in 0.1 mol·L ⁻¹ HCl	80	[9]
4 Alkyd resin containing MMO pigments: (TiO ₂ ·Fe ₂ O ₃), (TiO ₂ ·ZnO), (TiO ₂ ·NiO)	A36 steel in 3.5% NaCl	98.18 99.19 86.15	[10]
5 Alkyd resin coating containing titanium phosphates: Li _{0.5} M _{0.25} Ti ₂ (PO ₄) ₃ M = Mn, = Co = Ni	Carbon steel substrate in 3.5% sodium chloride solution	82.89 61.52 36.02	[11]
6 Our work: Alkyd resin with 3 mM Mg(GLY)	Carbon steel in 3.5% NaCl	97.12	Our work

The water uptake tests were performed in triplicate based on the EIS data, and the error bars represent the standard deviation. For the tested alkyd samples, water adsorption in the first 120 h of immersion in saline solution occurs through capillarity because of pores and/or micro-structural defects in the polymer film but also depends on the nature of the composition of the coating. The capacity of the polymer film (C) is a measure of water adsorption and permeability. Over time, the capacity of the polymer film usually increases due to water absorption. Determining the capacity of the polymer film for different times of immersion in electrolyte solutions, the volume fraction of absorbed water (W) was determined using the following equation based on the Brasher–Kingsbury Equation (2) [37].

$$W = \frac{\log[Ct/C_0]}{\log 80} \tag{2}$$

where W is the water volume fraction in the coating, ϵ_w is the dielectric constant of water ($\epsilon_w = 80$), and C_t and C_0 are the capacitance of the coating after a time t of immersion and at time $t = 0$ for the dry-coating capacitance.

The change in the capacitance of the coating related to water uptake is shown Figure 4a. The Nyquist plots in Figure 4a show the corrosion resistance of different alkyd samples after 120 h of immersion. The size of the semiarc in the plots indicates the level of corrosion resistance, with a larger diameter indicating better resistance. In comparison with carbon steel, all the alkyd samples have significantly larger semiarc diameters. This suggests that the alkyd coatings with an MOF provide higher corrosion resistance than carbon steel. Furthermore, for Alkyd 1, Alkyd 2, and Alkyd 3, the semiarc diameters are higher than those observed after one hour of immersion. This indicates that the corrosion resistance of these alkyd samples with MOFs improves over time.

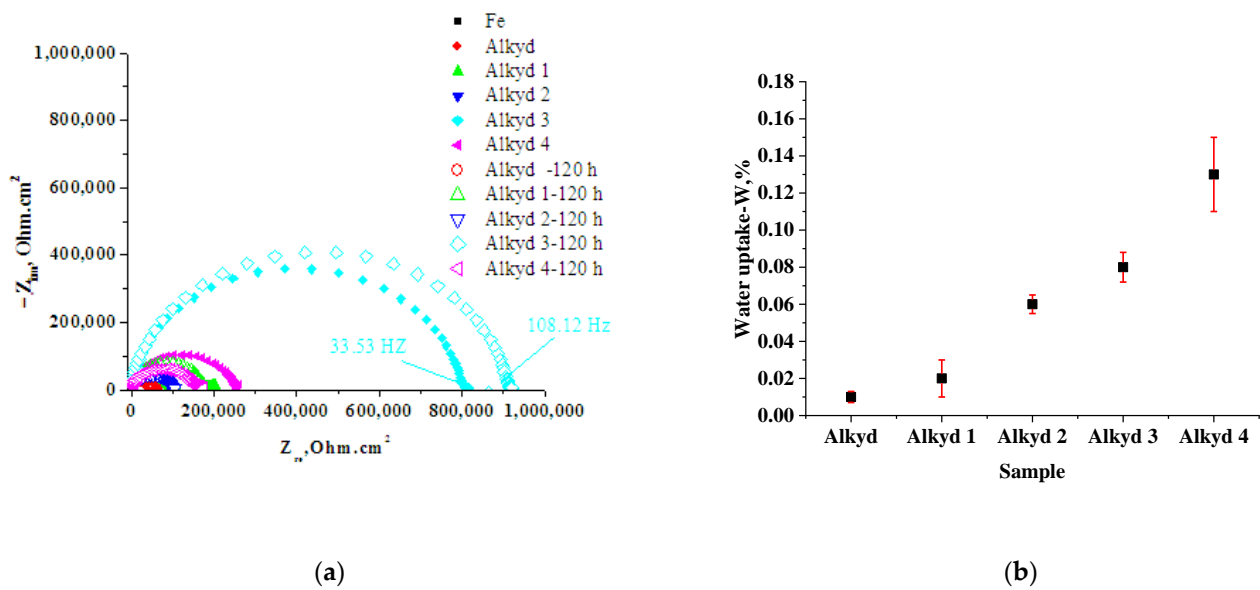


Figure 4. (a) Complex plane Nyquist plots for uncoated and coated carbon steel immersed for 120 h in 3.5% NaCl solutions and (b) water uptake of coatings. Error bars represent the standard deviation.

Overall, the Nyquist plots demonstrate that the alkyd coatings with an MOF have higher corrosion resistance compared with carbon steel, and this resistance improves with prolonged immersion.

The calculated R_1 values at an immersion time of 120 h are $2.01 \times 10^3 \pm 0.66 \times 10^2 \Omega \cdot \text{cm}^2$ for the metallic substrate, $8.24 \times 10^4 \pm 0.71 \times 10^1 \Omega \cdot \text{cm}^2$ for Alkyd, $2.87 \times 10^5 \pm 4.24 \times 10^1 \Omega \cdot \text{cm}^2$ for Alkyd 1, $3.75 \times 10^5 \pm 1.241 \times 10^2 \Omega \cdot \text{cm}^2$ for Alkyd 2, $8.03 \times 10^5 \pm 2.52 \times 10^2 \Omega \cdot \text{cm}^2$ for Alkyd 3, and $1.03 \times 10^5 \pm 2.57 \times 10^2 \Omega \cdot \text{cm}^2$ for Alkyd 4. The values of R_1 vary after exposure depending on the amount of MOF present in the alkyd. The slightly increased resistances observed for the Alkyd 1, Alkyd 2, and Alkyd 3 resins suggest that Mg(GLY) has the ability to form complexes that block the existing pores and limit the access of aggressive species to the metal surface, thus increasing the adherence of these coatings. According to the observations of Greenfield and Scantlebury [38], an organic cover generally provides good protection when its resistance is $10^8 \Omega \cdot \text{cm}^2$ or greater, and weak protection if its resistance is less than $10^6 \Omega \cdot \text{cm}^2$. The values obtained suggest that none of the alkyd layers behave promisingly, but it is worth noting the beneficial action of MOFs in limiting the decrease in coating resistance over time.

The water absorptions determined by EIS measurements were lower than 0.13 for all the polymer films, due to their hydrophobic character (Figure 4b). It was observed that the alkyd coating gave a lower W value, when compared with the alkyd-Mg(GLY) coatings. Indeed, the increase in Mg(GLY) content in the coating can lead to an increase in water permeability. The higher water absorption exhibited by the alkyd with Mg(GLY)

can be beneficial for the coating, as it allows the inhibitor to diffuse from the coating. A higher water uptake of coatings with Mg(GLY) up to a certain concentration (0.08 in this case) can be advantageous. Mg(GLY) facilitates the gradual release of the acid through its degradative hydrolysis, which can then complex with iron ions in the system, effectively blocking existing pores. Simultaneously, the released phosphonic groups can form new (P....O.....Fe) type bonds, further enhancing the adhesion of the film to the metal substrate and preventing the passage of water and corrosive ions throughout the coating layers. However, a higher water absorption, as observed in the case of Alkyd 4, would be unfavorable due to insufficiently blocked pores, compromising the protective properties of the coating. The coated steel specimen's images obtained by the optical microscope are shown in Figures 5 and 6.

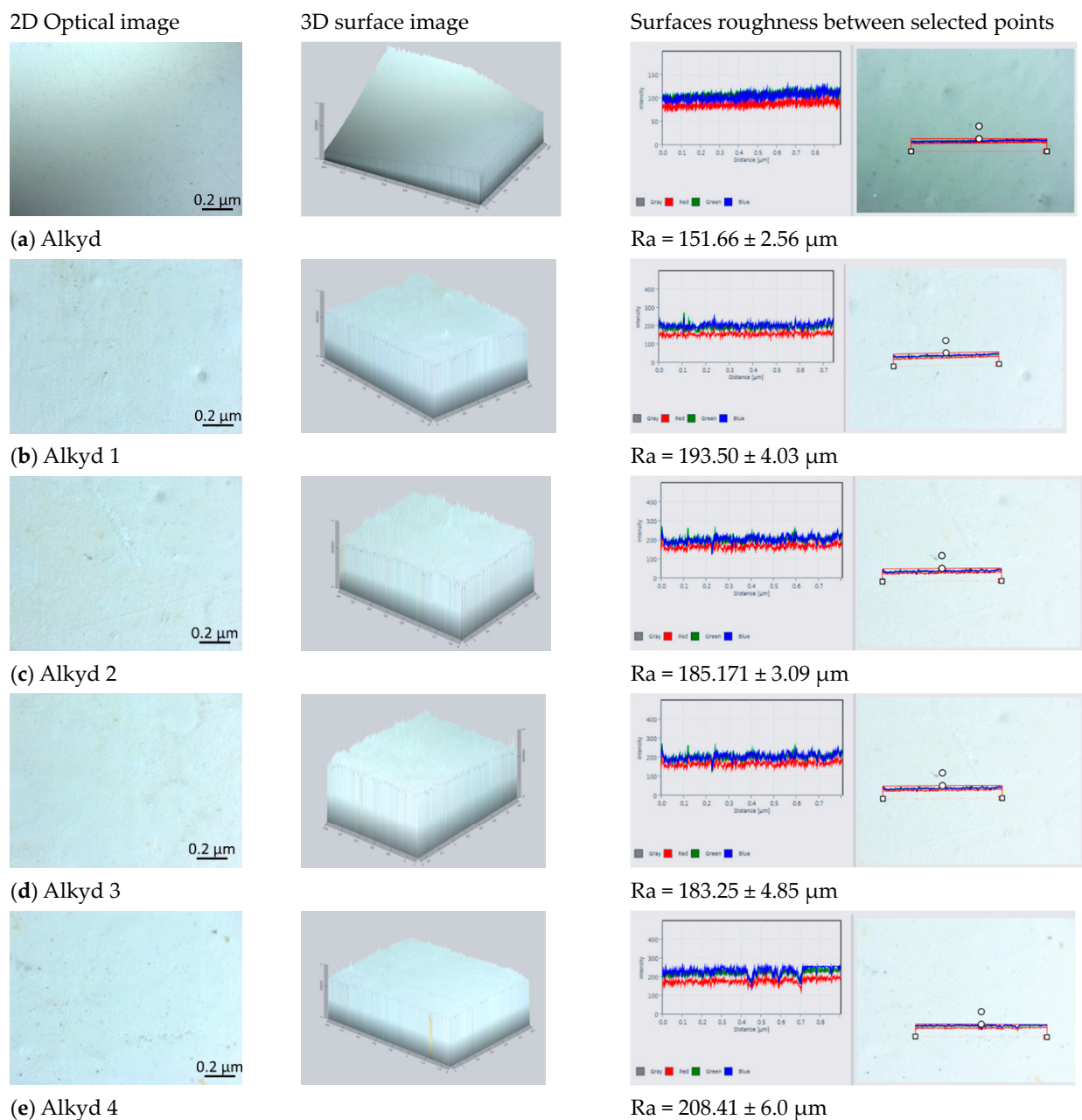


Figure 5. Coated steel alkyd specimen images: 2D and 3D optical microscope images and the roughness of surfaces (Ra) for (a) Alkyd, (b) Alkyd 1, (c) Alkyd 2, (d) Alkyd 3, and (e) Alkyd 4.

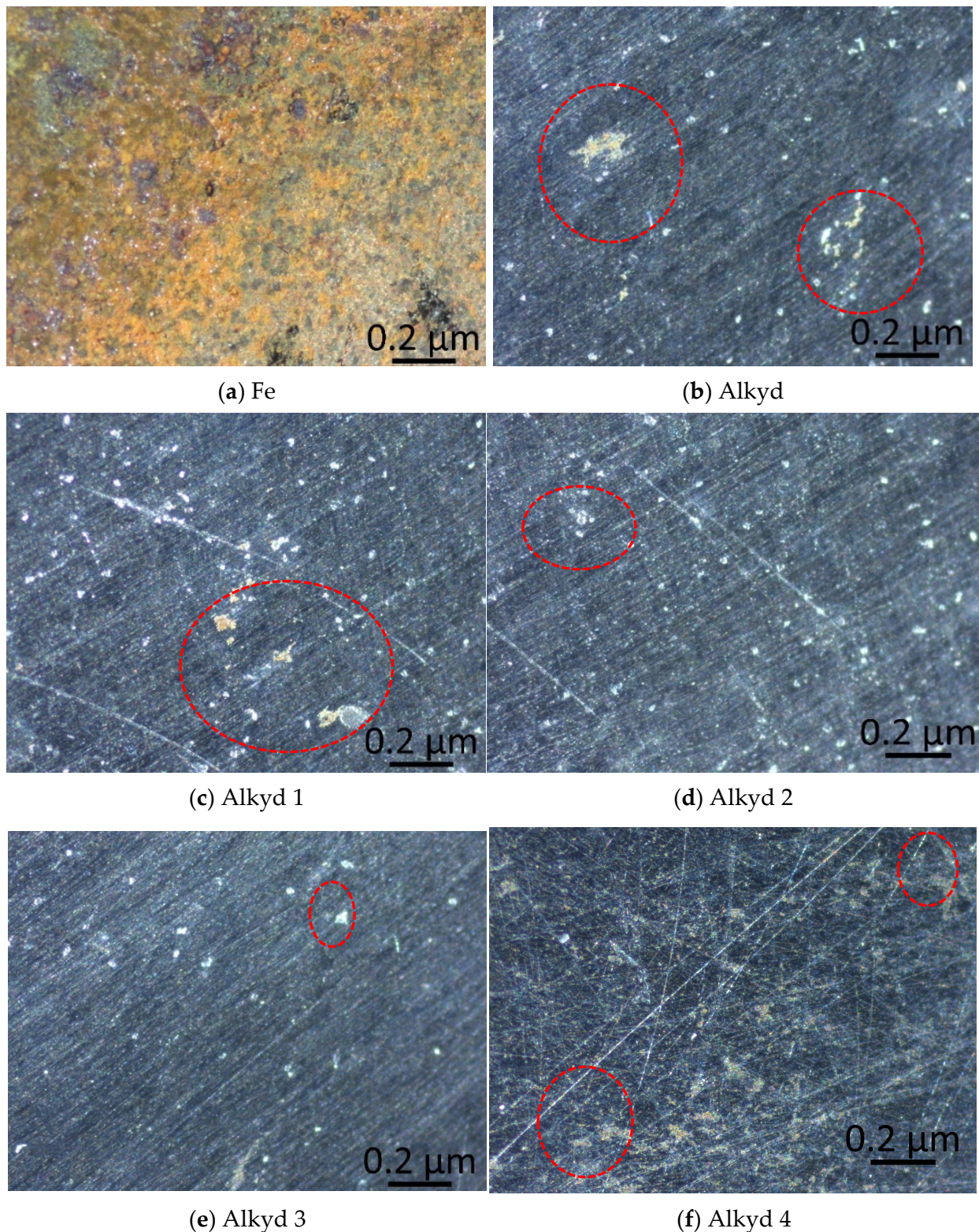


Figure 6. Carbon steel and coated steel alkyd specimen images obtained by optical microscope after 120 h of immersion in saline solution: (a) Fe, (b) Alkyd, (c) Alkyd 1, (d) Alkyd 2, (e) Alkyd 3, and (f) Alkyd 4.

The interaction between the phosphate group and the iron substrate suggests that the addition of Mg(GLY) in the alkyd composition acts as an inhibitor, gradually releasing free acid through hydrolytic degradation. This release of free acid enhances the performance of

the alkyd coating by improving adhesion, reducing coating delamination, and sealing of pores. It is worth noting that the Alkyd 4 coating appears to be less smooth, indicating the formation of a more porous coating at higher Mg(GLY) contents. Surface roughness can influence the corrosion behavior of carbon steel, which is consistent with the lower value of CPE1-P observed in the EIS data for Alkyd 4. On the other hand, the other alkyd samples exhibited increased smoothness, suggesting better performance. These changes can be attributed to the formation of a protective film that covers the surface, potentially reducing the active surface area susceptible to corrosion. The surface roughness Ra parameter (average roughness) was determined from the arithmetic average of the gray level, for three measurements on the same sample [36]. The improvement in smoothness for Alkyd 3 indicates higher performance. After the samples had been submerged in saline solution for 120 h, the samples' surfaces were also examined. With the aid of a solvent, the protective coatings were removed and allowed to dry for 2 h. Figure 6 displays the captured photos. Uncoated carbon steel exhibited significant amounts of corrosion products. The optical images in the case of iron reveal that after 120 h of immersion, corrosion products had substantially covered the carbon steel surface. In the case of Alkyd and Alkyd 1, some rust traces were present. This may be because, until the coating on metal surfaces cures fully, water can enter the metal surface through the built-in pores, leading to the appearance of rust. The film becomes more compact, durable, and corrosion-resistant after it has fully dried. The surface measurements by optical microscope showed an improvement in the surface smoothness in alkyd with Mg(GLY) additive, as shown in Figure 6. The absence of rust at more than 1 mM Mg(GLY) content in polyester resin suggests that a more durable and adherent coating had formed on the carbon steel. The greatest protection was seen at a concentration of 3 mM in alkyd.

The magnesium metal organic framework structure can be envisioned as a 2D layer structure. The majority of magnesium compounds prepared in hydrothermal aqueous media contain water molecules coordinating with the metallic centre. The coordination geometry of the Mg centre is a distorted octahedral (Table 1). Each individual layer is formed by Mg–O(phosphonate) bonds, forming 16-membered rings. The carboxylic moiety (–COO–) is deprotonated but it is non-coordinating to the metallic centre. This moiety is prolonged into the interlayer region and is responsible in the formation of the wavy motif [26,27,32,34]. The mechanism of action involves the ability of Mg(GLY) to retain the Fe²⁺ cations that have already formed as a result of the corrosive environment, as well as the ability of the released GLY acid to do the same (via COOH groups or P(O)(OH)₂). In a corrosive environment, the Fe²⁺ cations present due to metal oxidation can be retained by these carboxylic groups to form a complex (Figure 7a,c). These complexes block the existing pores and limit the access of aggressive species at the metallic surface. By diffusion in the existing pores in the alkyd coating, the hydrated ions reach the vicinity of the Mg(GLY) molecules (Figure 7a,b).

In addition to this form of complexation, hydrolytic degradation is able to take place. The metal–O–P bonds can break and the phosphonate ligands are released as free phosphonic acid. Free phosphonic acid can also form complexes with the Fe ions resulting from the corrosion process and/or bind in a well-known manner to the metal surface (Figure 7a,c) in a mono, bi or tridentate way [27,39–41]. In this mode, the release of phosphonic acid prevents corrosion, by increasing the compactness and adhesion of the coating (P.....O.....Me) and by sealing the existing pores with complexes (Figure 7d). The metallic surface affinity of the phosphonic groups plays an important role in the formation of the protective layer, and the binding mode can be responsible for the compactness and adherence of the layer, eliminating the need for a primer layer, which can save time and money by allowing direct application.

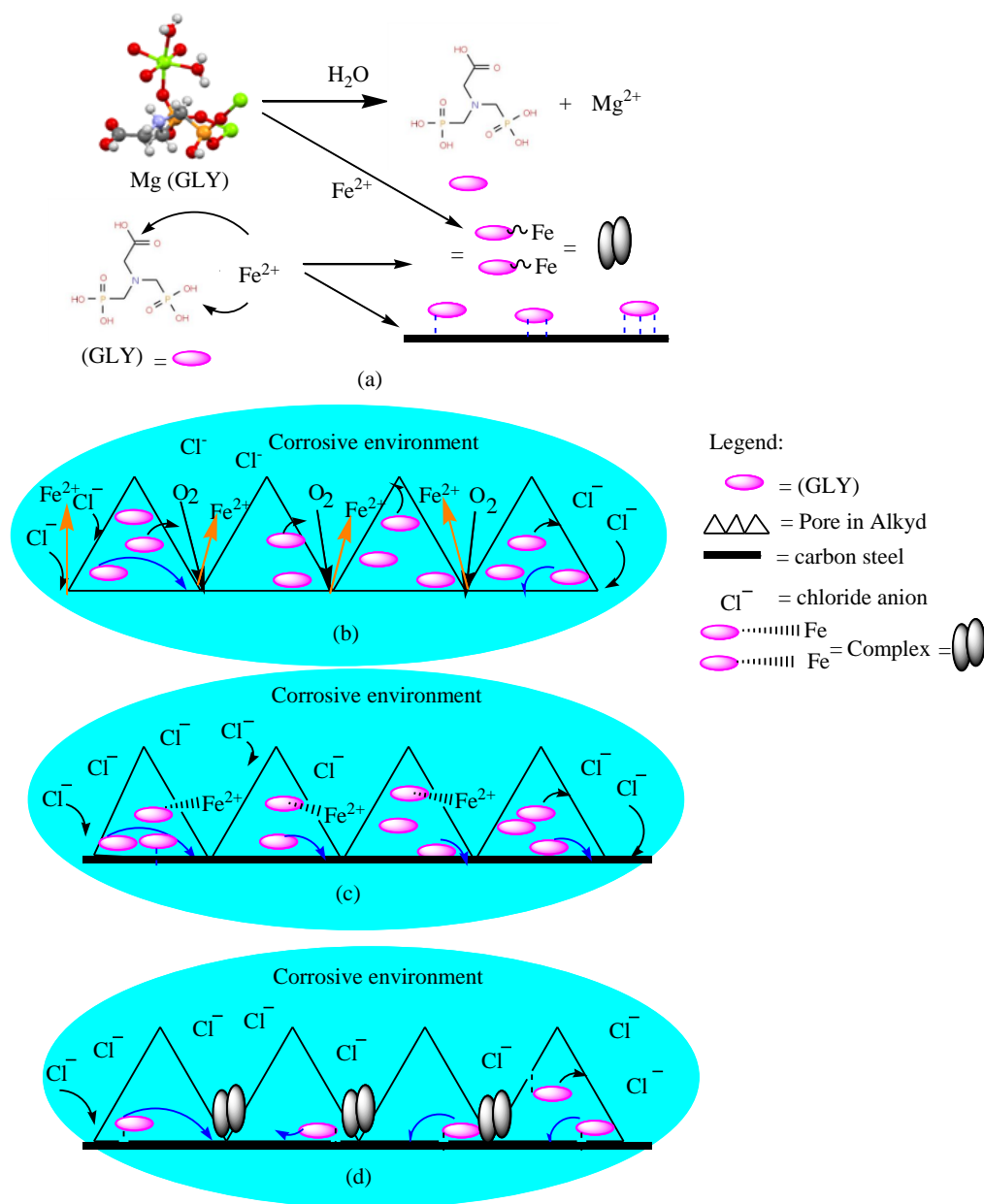


Figure 7. (a) Complexation mode on carbon steel surface; (b) hydrolytic degradation of Mg(GLY) with the release of free acid; (c) complexation with the existing cations in the system; and (d) blocking of the existing pores in the coating. Mg²⁺, Na⁺ and H⁺ are omitted for clarity.

4. Conclusions

Polyester with a 49% oil content, prepared using fatty acids from soybeans, phthalic anhydride and pentaerythritol, can be synthesized under microwave irradiation. The utilization of phthalic anhydride and pentaerythritol in the synthesis process contributes to the formation of a cross-linked network within the polyester, resulting in increased resistance to corrosion and damage from external factors. The combination of these specific components and synthesis method contributes to the improved performance of the polyester. The high oil content from soybean fatty acids provides better film-forming and adhesion properties, enhancing the durability and protective capabilities of the alkyd coating. (Mg(GLY)) is known for its corrosion inhibition properties, and its inclusion in the polyester formulation helps to prevent the onset and progression of corrosion on the coated surface. The incorporation of 3 mM Mg(GLY) further enhances the anticorrosive properties of the alkyd coating.

The interaction between the alkyd resin, the MOF additive and iron cations is facilitated through the acid groups (COOH or PO(OH)₂) and with the iron surface via double bonds, P=O, and P-OH groups. This interaction was confirmed by electrochemical tests and optical microscopy. The most satisfactory protection for carbon steel was achieved with an Mg(GLY) concentration of 3 mM, exhibiting an inhibition efficiency of approximately 97%, the highest polarization resistance value and the lowest double layer capacitance values. These results suggest reduced coating delamination and improved barrier properties, effectively blocking defects. Overall, the combination of these components and synthesis method results in a polyester with superior anticorrosive properties, making it an excellent choice for alkyd coatings in applications where protection against corrosion is crucial.

The promising results obtained with the alkyd resin containing the Mg(GLY) additive suggest that this type of resin can be directly applied for the protection of iron without the need for a primer layer. This not only brings economic benefits but also saves time. Further research is recommended to investigate the long-term behavior and accelerated aging of these coatings under UV exposure.

Author Contributions: Conceptualization, D.J. and N.P.; methodology, D.J., L.M. and A.V.; validation, B.M. and A.V.; formal analysis, M.T.-L.M., L.M. and N.P.; investigation, D.J., L.M. and N.P.; resources, D.J.; data curation, B.M., A.V., M.T.-L.M. and N.P.; writing—original draft preparation, review and editing, N.P. and A.V.; supervision, D.J. and N.P. All authors have read and agreed to the published version of the manuscript.

Funding: This work was partially supported by the project “ICT—Interdisciplinary Center for Smart Specialization in Chemical Biology (RO-OPENSSCREEN)”, MySMIS code: 127952, Contract no. 371/20.07.2020, co-financed by the European Regional Development Fund under the Competitiveness Operational Program 2014–2020, and partially supported by the “Coriolan Dragulescu” Institute of Chemistry, Program 2.

Data Availability Statement: Not applicable.

Acknowledgments: The authors are deeply grateful SC Elkim Special SRL.

Conflicts of Interest: The authors declare no conflict of interest.

References

1. Lyon, S.B.; Bingham, R.; Mills, D.J. Advances in corrosion protection by organic coatings: What we know and what we would like to know. *Prog. Org. Coat.* **2017**, *102*, 2–7. [[CrossRef](#)]
2. Agbo, C.; Jakpa, W.; Sarkodie, B.; Boakye, A.; Fu, S. A Review on the Mechanism of Pigment Dispersion. *J. Dispers. Sci.* **2017**, *39*, 874–889. [[CrossRef](#)]
3. Njoku, C.N.; Bai, W.; Arukalam, I.O.; Yang, L.; Hou, B.; Njoku, D.I.; Li, Y. Epoxy-based smart coating with self-repairing polyurea-formaldehyde microcapsules for anticorrosion protection of aluminum alloy AA2024. *J. Coat. Technol. Res.* **2020**, *17*, 797–813. [[CrossRef](#)]
4. Njoku, C.N.; Arukalam, I.O.; Bai, W.; Li, Y. Optimizing Maleic Anhydride Microcapsules Size for Use in Self-healing Epoxy-Based Coatings for Corrosion Protection of Aluminum Alloy. *Mater. Corros. Werkst. Korros.* **2018**, *69*, 1257–1267. [[CrossRef](#)]
5. Boga, K.; Pothu, R.; Arukula, R.; Boddula, R.; Kumar Gaddam, S. The role of anticorrosive polymer coatings for the protection of metallic surface. *Corros. Rev.* **2021**, *39*, 547–559. [[CrossRef](#)]
6. Plesu, N.; Ilia, G.; Pascariu, A.; Vlase, G. Preparation, degradation of polyaniline doped with organic phosphorus acids and corrosion essays of polyaniline–acrylic blends. *Synth. Met.* **2006**, *156*, 230–238. [[CrossRef](#)]
7. Abdou, M.I.; El-Sayed Ahmed, H.; Wahab Gaber, M.A.; Fadl, A.M. Enhancement of anti-corrosion and mechanical properties of alkyd-based protective paints for steel petroleum structures incorporating natural limonite pigment. *Cogent Eng.* **2018**, *5*, 1427844. [[CrossRef](#)]
8. Deyab, M.A.; Słota, R.; Bloise, E.; Mele, G. Exploring corrosion protection properties of alkyd@lanthanide bis-phthalocyanine nanocomposite coatings. *RSC Adv.* **2018**, *8*, 1909–1916. [[CrossRef](#)]
9. Mousa, O.I.; Al-Luaibi, S.S.; Al-Mubarak, A.S.; Lgaz, H.; Hammouti, B.; Chaouiki, A.; Gun Ko, Y. On the Development of an Intelligent Poly(aniline-co-o-toluidine)/Fe₃O₄/Alkyd Coating for Corrosion Protection in Carbon Steel. *Appl. Sci.* **2023**, *13*, 8189. [[CrossRef](#)]
10. Benitha, V.S.; Jeyasubramanian, K.; Hikku, G.S. Investigation of anti-corrosion ability of nano mixed metal oxide pigment dispersed alkyd coating and its optimization for A36 steel. *J. Alloys Compd.* **2017**, *721*, 563–576. [[CrossRef](#)]

11. Deyab, M.A.; Eddahaoui, K.; Essehli, R.; Benmokhtar, S.; Rhadfi, T.; De Riccardis, A.; Mele, G. Influence of newly synthesized titanium phosphates on the corrosion protection properties of alkyd coating. *J. Mol. Liq.* **2016**, *216*, 699–703. [CrossRef]
12. Bao, Y.; Yan, Y.; Chen, Y.; Ma, J.; Zhang, W.; Liu, C. Facile fabrication of BTA@ZnO microcapsules and their corrosion protective application in waterborne polyacrylate coatings. *Prog. Org. Coat.* **2019**, *136*, 105233. [CrossRef]
13. Rössler, J.; Martin, U.; Bosch, J.; Bastidas, D.M. pH-Triggered release of NaNO₂ corrosion inhibitors from novel colophony microcapsules in simulated concrete pore solution. *ACS Appl. Mater. Interfaces* **2020**, *12*, 46686–46700. [CrossRef] [PubMed]
14. Söylev, T.A.; Richardson, M.G. Corrosion inhibitors for steel in concrete: State-of-the-art report. *Constr. Build. Mater.* **2008**, *22*, 609–622. [CrossRef]
15. González, E.; Stühr, R.; Vega, J.M.; García-Lecina, E.; Grande, H.-J.; Leiza, J.R.; Paulis, M. Assessing the effect of CeO₂ nanoparticles as corrosion inhibitor in hybrid biobased waterborne acrylic direct to metal coating binders. *Polymers* **2021**, *13*, 848. [CrossRef]
16. Chimenti, S.; Vega, J.M.; García-Lecina, E.; Grande, H.-J.; Paulis, M.; Leiza, J.R. In-situ phosphatization and enhanced corrosion properties of films made of phosphate functionalized nanoparticles. *React. Funct. Polym.* **2019**, *143*, 104334. [CrossRef]
17. Hao, Y.; Sani, L.A.; Ge, T.; Fang, Q. Phytic acid doped polyaniline containing epoxy coatings for corrosion protection of Q235 carbon steel. *Appl. Surf. Sci.* **2017**, *419*, 826–837. [CrossRef]
18. Wang, H.; Di, D.; Zhao, Y.; Yuan, R.; Zhu, Y. A multifunctional polymer composite coating assisted with pore-forming agent: Preparation, superhydrophobicity and corrosion resistance. *Prog. Org. Coat.* **2019**, *132*, 370–378. [CrossRef]
19. Pan, S.; Wang, N.; Xiong, D.; Deng, Y.; Shi, Y. Fabrication of superhydrophobic coating via spraying method and its applications in anti-icing and anticorrosion. *Appl. Surf. Sci.* **2016**, *389*, 547–553. [CrossRef]
20. Motlatle, A.M.; Ray, S.S.; Ojijo, V.; Scriba, M.R. Polyester-Based Coatings for Corrosion Protection. *Polymers* **2022**, *14*, 3413. [CrossRef]
21. Hasniraiman, A.H.; Zuliahani, A.; Ishak, M.; Faiza, M.A.; Azniwati, A.A. Comparison studies on corrosive properties of polyester filled graphene primer coatings via sonication and mechanical method. *Prog. Color Color. Coat.* **2019**, *12*, 211–218.
22. Tsai, P.-Y.; Chen, T.-E.; Lee, Y.-L. Development and Characterization of Anticorrosion and Antifriction Properties for High Performance Polyurethane/Graphene Composite Coatings. *Coatings* **2018**, *8*, 250. [CrossRef]
23. Gadipelli, S.; Ford, J.; Zhou, W.; Wu, H.; Udovic, T.J.; Yildirim, T. Nanoconfinement and Catalytic Dehydrogenation of Ammonia Borane by Magnesium-Metal-Organic-Framework-74. *Chem. Eur. J.* **2011**, *17*, 6043. [CrossRef]
24. Williams, C.A.; Blake, A.J.; Wilson, C.; Hubberstey, P.; Schröder, M. Novel metal-organic frameworks derived from group II metal cations and aryldicarboxylate anionic ligands. *Cryst. Growth Des.* **2008**, *8*, 911–922. [CrossRef]
25. Umida, K.; Brown, C.M.; Herm, Z.R.; Chavan, S.; Bordiga, S.; Long, J.R. Hydrogen storage properties and neutron scattering studies of Mg₂(dobdc)-A metal-organic framework with open Mg²⁺ adsorption sites. *Chem. Commun.* **2011**, *47*, 1157–1159. [CrossRef]
26. Demadis, K.D.; Famelis, N.; Cabeza, A.; Aranda, M.A.G.; Colodrero, R.M.P.; Infantes-Molina, A. 2D Corrugated Magnesium Carboxyphosphonate Materials: Topotactic Transformations and Interlayer “Decoration” with Ammonia. *Inorg. Chem.* **2012**, *51*, 7889. [CrossRef] [PubMed]
27. Maranescu, B.; Lupa, L.; Tara-Lunga Mihali, M.; Plesu, N.; Maranescu, V.; Visa, A. The corrosion inhibitor behavior of iron in saline solution by the action of magnesium carboxyphosphonate. *Pure Appl. Chem.* **2018**, *90*, 1713–1722. [CrossRef]
28. Ingold, C.K. *Structure and Mechanism in Organic Chemistry*; Cornell University Press: Ithaca, NY, USA, 1969; p. 1129. ISBN 10: 0-801-40499-1.
29. Smith, M.B.; March, J. *March's Advanced Organic Chemistry, Reaction Mechanism and Structure*, 6th ed.; John Wiley & Sons, Inc.: New Jersey, NY, USA, 2007; p. 398. ISBN 10: 0-471-72091-7. Available online: <https://rushim.ru/books/mechanizms/march6ed.pdf> (accessed on 10 June 2023).
30. Nouigues, A.; Le Gal La Salle, E.; Bailleul, J.L. Thermo-mechanical characterization of unsaturated polyester/glass fiber composites for recycling. *Int. J. Mater. Form.* **2021**, *14*, 153–174. [CrossRef]
31. Bacaloglu, R.; Fisch, M.; Biesiada, K. Kinetics of polyesterification of adipic acid with 1,3-butanediol. *Polym. Eng.* **1998**, *38*, 1014–1022. [CrossRef]
32. Strauss, C.R.; Rooney, D.W. Accounting for clean, fast and high yielding reactions under microwave conditions. *Green Chem.* **2010**, *12*, 1340–1344. [CrossRef]
33. Brug, G.J.; Van Den Eedem, A.L.G.; Sluyters Rechbach, M.; Sluyters, J.H. The analysis of electrode impedances complicated by the presence of a constant phase element. *J. Electroanal. Chem. Interfacial Electrochem.* **1984**, *176*, 275–295. [CrossRef]
34. Marchebois, H.; Touzain, S.; Joiret, S.; Bernard, J.; Savall, C. Zinc-rich powder coatings corrosion in sea water: Influence of conductive pigments. *Prog. Org. Coat.* **2002**, *45*, 415–421. [CrossRef]
35. Huang, B.-S.; Lai, G.-H.; Yang, T.-I.; Tsai, M.-H.; Chou, Y.-C. A novel electroactive imide oligomer and its application in anticorrosion coating. *Polymers* **2020**, *12*, 91. [CrossRef] [PubMed]
36. Molina, J.; Puig, M.; Gimeno, M.; Izquierdo, R.; Gracenea, J.; Suay, J. Influence of zinc molybdenum phosphate pigment on coatings performance studied by electrochemical methods. *Prog. Org. Coat.* **2016**, *97*, 244–253. [CrossRef]
37. Brasher, D.M.; Kingsbury, A.H. Electrical measurements in the study of immersed paint coatings on metal. I. Comparison between capacitance and gravimetric methods of estimating water-uptake. *J. Appl. Chem.* **1954**, *62*, 62–67. [CrossRef]
38. Greenfield, D.; Scantlebury, D. The protective action of organic coatings on steel: A review. *J. Corros. Sci. Eng.* **2000**, *3*, 1–13.

39. Moschona, A.; Plesu, N.; Colodrero, R.M.P.; Cabeza, A.; Thomas, A.G.; Demadis, K.D. Homologous alkyl side-chain diphosphate inhibitors for the corrosion protection of carbon steels. *Chem. Eng. J.* **2021**, *405*, 126864. [[CrossRef](#)]
40. Maranescu, B.; Plesu, N.; Visa, A. Phosphonic acid vs phosphonate metal organic framework influence on mild steel corrosion protection. *Appl. Surf. Sci.* **2019**, *497*, 143734. [[CrossRef](#)]
41. Visa, A.; Mracec, M.; Maranescu, B.; Ilia, G.; Popa, A.; Mracec, M. Structure simulation into a lamellar supramolecular network and calculation of the metal ions/ligands ratio. *Chem. Cent. J.* **2012**, *6*, 91. [[CrossRef](#)]

Disclaimer/Publisher's Note: The statements, opinions and data contained in all publications are solely those of the individual author(s) and contributor(s) and not of MDPI and/or the editor(s). MDPI and/or the editor(s) disclaim responsibility for any injury to people or property resulting from any ideas, methods, instructions or products referred to in the content.